

Efficient CO₂ Capture by a 3D Porous Polymer Derived from Tröger's Base

Xiang Zhu,^{†,‡} Chi-Linh Do-Thanh,[§] Christopher R. Murdock,[§] Kimberly M. Nelson,[§] Chengcheng Tian,^{†,‡} Suree Brown,[§] Shannon M. Mahurin,[‡] David M. Jenkins,[§] Jun Hu,[†] Bin Zhao,[§] Honglai Liu,^{*,†} and Sheng Dai^{*,‡,§}

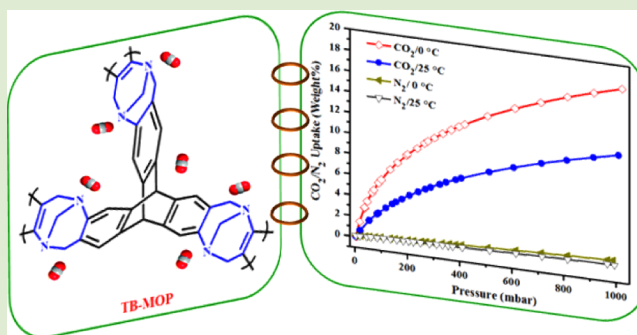
[†]State Key Laboratory of Chemical Engineering and Department of Chemistry, East China University of Science and Technology, Shanghai 200237, China

[‡]Chemical Science Division, Oak Ridge National Laboratory, 1 Bethel Valley Road, Oak Ridge, Tennessee 37831, United States

[§]Department of Chemistry, The University of Tennessee, Knoxville, Tennessee 37996-1600, United States

S Supporting Information

ABSTRACT: A 3D Tröger's-base-derived microporous organic polymer with a high surface area and good thermal stability was facilely synthesized from a one-pot metal-free polymerization reaction between dimethoxymethane and triaminotriptycene. The obtained material displays excellent CO₂ uptake abilities as well as good adsorption selectivity for CO₂ over N₂. The CO₂ storage can reach up to 4.05 mmol g⁻¹ (17.8 wt %) and 2.57 mmol g⁻¹ (11.3 wt %) at 273 K and 298 K, respectively. Moreover, the high selectivity of the polymer toward CO₂ over N₂ (50.6, 298 K) makes it a promising material for potential application in CO₂ separation from flue gas.



Carbon capture and sequestration (CCS), a newly emerged strategy to mediate the atmospheric CO₂ concentration for environmental remediation, has attracted significant interest.^{1,2} Conventional processes widely employed in industry for CO₂ capture involve chemical absorption of CO₂ with ethanolamine solutions. Though this method is well-established and offers a high CO₂ absorption capacity, it suffers from several serious drawbacks, including solvent loss, a high parasitic energy cost for the regeneration, and equipment corrosion.³ Therefore, alternative processes such as adsorption separation by porous solid-adsorbents have been proposed.^{4–13}

Recently, tremendous attention has been paid to the design and synthesis of microporous organic polymers (MOPs) for CO₂ capture due to their high physicochemical stability and excellent adsorption capacity.^{1,2,14–31} Numerous MOPs with good porosities (both surface areas and pore volumes) have been prepared via a variety of organic reactions. Several potential strategies like increasing isosteric heats between sorbent and sorbate have been developed to increase CO₂ loading capacity and the adsorption selectivity for CO₂ over N₂, which is another crucial parameter for CO₂ capture materials.³² In this regard, various CO₂-philic moieties have been incorporated into the porous polymer networks to enhance the interaction between the material surfaces and CO₂ molecules. Typically, grafting of one ultrahigh-surface-area network (PPN-6) with sulfonic acid, lithium sulfonate, or polyamines attains excellent CO₂ adsorption capacities as well

as high CO₂/N₂ selectivity.^{1,2} In spite of these beneficial properties, multistep synthesis processes of such attractive adsorbents may limit the scale-up preparation for CO₂ capture. Facile and cost-effective preparation processes combined with excellent gas adsorption properties are the keys to make MOPs as promising candidates for practical applications in post-combustion capture of CO₂.

With these considerations in mind, herein we report the one-pot metal-free synthesis of a three-dimensional (3D) Tröger's-base-derived microporous organic polymer (TB-MOP, Scheme 1) for efficient CO₂ capture. The resulting network showed excellent CO₂ uptake as well as high adsorption selectivity for CO₂ over N₂ at ambient conditions.

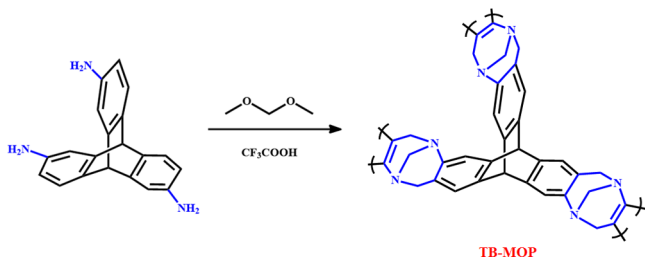
TB-MOP was prepared through a trifluoroacetic acid-catalyzed one-pot polymerization reaction between dimethoxymethane and a 3D rigid building block (triaminotriptycene) at room temperature (Scheme 1). CO₂-philic TB units can be facilely in situ generated. This synthesis was inspired by the recent discovery of porous TB based membranes.³³ 2,6,14-Triaminotriptycene, which may allow for a high degree of internal molecular free volume,²⁴ was selected as the precursor for our polymer network synthesis and can easily be prepared from triptycene in good yield.³⁴ (Experimental details can be

Received: July 3, 2013

Accepted: July 11, 2013

Published: July 16, 2013

Scheme 1. Synthesis of TB-MOP at Room Temperature



found in the Supporting Information.) The resulting 3D TB-MOP was found to be insoluble in common organic solvents.

The structure of TB-MOP can be characterized at the molecular level by solid state ^{13}C cross-polarization magic-angle spinning (CP/MAS) NMR (Figure 1A). The existences of in situ generated TB units within the network are confirmed by the signals at ca. 55, 68, 111, 124, and 146 ppm.^{35,36} The peak at 136 ppm corresponds to carbon atoms of the substituted benzene rings.^{35,36} High thermal stability of TB-MOP was revealed by thermogravimetric analysis (TGA, Figure S1). TB-MOP retains more than 60% of its mass at 800 °C under N_2 atmosphere. It is worth mentioning that high thermal stabilities of MOPs are beneficial for considering their potential application in postcombustion processes at higher temperatures and CO_2 scrubbing operations.^{30,37} Moreover, TB-MOP is shown to be amorphous as indicated by X-ray powder diffraction measurement (Figure S2), which is similar to previous triptycene derived MOPs.^{24,35}

The porosity of TB-MOP was evaluated by a nitrogen adsorption isotherm measured at 77 K (Figure 1B), which exhibited a Type I adsorption profile. A rapid uptake at low pressure (0–0.1 bar) indicated a permanent microporous

nature of the polymeric network. The calculated Brunauer–Emmett–Teller (BET) surface area is shown to be $\sim 694 \text{ m}^2 \text{ g}^{-1}$ and can be comparable to that reported for conjugated microporous polymer-derived adsorbents.¹⁸ The level of microporosity in the material was assessed by the ratio of micropore volume to the total pore volume ($V_{\text{micro}}/V_{\text{total}}$).³⁸ The total pore volume (calculated at $P/P_0 \sim 0.98$) and micropore volume derived from the t-plot method were $0.398 \text{ cm}^3 \text{ g}^{-1}$ and $0.179 \text{ cm}^3 \text{ g}^{-1}$, respectively. For TB-MOP, a $V_{\text{micro}}/V_{\text{total}}$ value of 0.45 was obtained, indicating the existence of mesopores.²⁸ Moreover, the pore size distribution (PSD) analysis based on nonlocal density functional theory (NLDFT) further confirmed the presence of primarily micropores with a small mesopore contribution (Figure 1B). The presence of mesopores may be a result of the intrinsic porosity and expanded networks of the 3D rigid building blocks.³⁵

In view of the fact that TB-MOP possesses two key properties of high CO_2 uptake capacity, for example, good microporosity and abundant nitrogen-containing CO_2 -philic sites, the CO_2 adsorption of TB-MOP was measured up to 1 bar (Figure 1C) using a gravimetric microbalance (IGA, Hiden Isochema). Uptakes of 4.05 mmol g^{-1} (17.8 wt %) and 2.57 mmol g^{-1} (11.3 wt %) were obtained at 273 and 298 K, respectively. To directly compare CO_2 capture performance for different MOPs, we have plotted the CO_2 uptake at both 273 and 298 K and 1 bar for a range of MOP-based adsorbents as a function of BET surface area measured by N_2 adsorption at 77 K (Figure S3A and B). TB-MOP, as can be seen, shows a higher CO_2 adsorption capacity than many previously reported MOPs under the same conditions despite possessing a lower BET surface area (Table S1).³² Moreover, although benzimidazole-linked polymers with higher surface areas show better CO_2 uptake (filled circles in Figure S3A and B), the preparation of their building blocks are more challenging than our facile

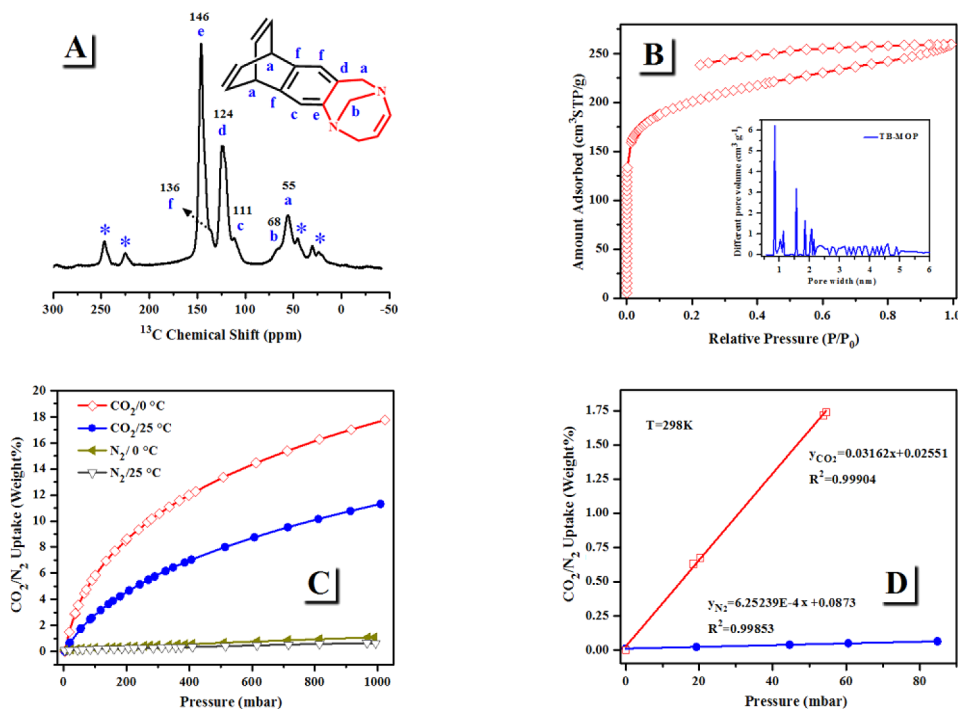


Figure 1. (A) Solid state ^{13}C -CP/MAS NMR spectrum of TB-MOP. The asterisk denotes spinning sidebands. (B) Nitrogen gas adsorption isotherms measured at 77 K and corresponding pore size distribution curve (inset) of TB-MOP. (C) CO_2 and N_2 adsorption isotherms of TB-MOP measured at 273 and 298 K. (D) Initial slope calculation for CO_2 and N_2 isotherms collected at 298 K.

synthesis.^{24–26} Previous work has shown that CO₂-philic sites such as acid groups and N-containing heterocyclic rings may have a large effect on CO₂ uptake besides the contribution of porosity (surface area and pore volume).¹⁸ To provide a better understanding of the CO₂ storage properties, the isosteric heat of adsorption for TB-MOP was calculated by fitting the CO₂ adsorption isotherms measured at 273 and 298 K and applying a variant of the Clausius–Clapeyron equation (see Supporting Information).¹¹ TB-MOP shows a heat in the range of 24.5–29.5 kJ mol⁻¹ (Figure S4). This value is higher than that reported for many other MOPs.³² However, the value still remains below the energy of chemisorptive processes (>40 kJ mol⁻¹),³⁰ indicating strong interactions of the polarizable CO₂ molecules through dipole–quadrupole interactions with the network, along with the inherent microporosity of TB-MOP, which is more favorable for facile CO₂ desorption. The readily reversible adsorption/desorption behavior (Figure S5) further indicates that interactions between CO₂ molecules and TB-MOP are weak enough to allow for adsorbent regeneration without applying heat.²⁶ Additionally, CO₂ uptake at 10 bar for TB-MOP was measured to be 8.39 mmol g⁻¹ (36.9 wt %, 273 K) and 6.18 mmol g⁻¹ (27.2 wt %, 298 K), respectively, showing good adsorption abilities at high pressure (see Figure S5).

Inspired by the excellent CO₂ uptake abilities and high isosteric heat for TB-MOP, N₂ adsorption experiments were carried out at 1 bar to examine the separation capability since industrial emission stream also contains ~70% N₂ (see Figure 1C). The selectivity for CO₂ over N₂ was calculated to be 45.2 at 273 K by the ratios of the initial slopes of CO₂ and N₂ adsorption isotherms (Figure S6),²² indicating increased selectivity as compared to previously reported MOPs. For example, much smaller CO₂/N₂ selectivity (25) at 273 K for carbazole-based porous organic polymer is observed though it possesses a higher CO₂ loading capacity (21.2 wt %, 273 K).²¹ Interestingly, at a higher temperature (298 K), the selectivity for TB-MOP was shown to be even larger and increased to 50.6 (Figure 1D). A similar trend has recently been indicated in N₂-phobic azo-based MOPs.³⁰ It should be noted that the CO₂/N₂ selectivity as well as CO₂ uptakes for many MOPs have been reported only at 273 K though CO₂/N₂ separation at the higher temperature of 298 K is closer to the conditions required for postcombustion capture.¹⁷ Accordingly, the in situ generated TB units within the network may play a role similar as the azo group, leading to a higher CO₂/N₂ selectivity at 298 K. The stronger affinity between CO₂ molecules and TB-MOP can be ascribed to the enhanced dipole–quadrupole interaction between the large quadrupole moment of CO₂ molecules (-1.4×10^{-39} C m²) and the polar TB sites.²² Moreover, given the effect of water on CO₂ uptake process,²³ a water droplet was brought in contact with the surface of a mechanically compressed TB-MOP thin pellet for the contact angle (CA) measurement.³⁹ However, the CA could not be obtained because, upon touching the pellet, the water droplet was absorbed immediately by TB-MOP. This indicates that the selectivity of TB-MOP toward CO₂ over N₂ will likely be affected by the presence of water under more realistic carbon capture conditions.

In conclusion, a 3D Tröger's-base-derived microporous organic polymer with a high surface area and good thermal stability can be facilely synthesized from a one-pot metal-free polymerization reaction between dimethoxymethane and triaminotriptycene. The obtained material displays excellent

CO₂ uptake abilities as well as high adsorption selectivity for CO₂ over N₂. The CO₂ storage can reach up to 4.05 mmol g⁻¹ (17.8 wt %) and 2.57 mmol g⁻¹ (11.3 wt %) at 273 K and 298 K, respectively, which can be competitive with many other CO₂ adsorbents. Moreover, the high selectivity of the polymer toward CO₂ over N₂ (50.6, 298 K) makes it a promising material for potential application in CO₂ separation from flue gas. Work on expansion of triptycene derived materials along with Tröger's base units for membrane based CO₂/N₂ separation is currently underway in our lab.

■ ASSOCIATED CONTENT

📄 Supporting Information

Synthesis details, gas adsorption experiments, Figures S1–S9, and Table S1. This material is available free of charge via the Internet at <http://pubs.acs.org>.

■ AUTHOR INFORMATION

Corresponding Author

*E-mail: hlliu@ecust.edu.cn; dais@ornl.gov.

Notes

The authors declare no competing financial interest.

■ ACKNOWLEDGMENTS

We are grateful to the financial support from the Division of Chemical Sciences, Geosciences, and Biosciences, Office of Basic Energy Sciences, U.S. Department of Energy. X.Z., C.C.T., J.H., and H.L.L. thank the National Basic Research Program of China (2013CB733501), the National Natural Science Foundation of China (No. 20990224, 21176066), the 111 Project of China (No. B08021), and the Fundamental Research Funds for the Central Universities of China.

■ REFERENCES

- (1) Lu, W.; Yuan, D.; Sculley, J.; Zhao, D.; Krishna, R.; Zhou, H.-C. *J. Am. Chem. Soc.* **2011**, *133*, 18126–18129.
- (2) Lu, W.; Sculley, J. P.; Yuan, D.; Krishna, R.; Wei, Z.; Zhou, H.-C. *Angew. Chem., Int. Ed.* **2012**, *51*, 7480–7484.
- (3) D'Alessandro, D. M.; Smit, B.; Long, J. R. *Angew. Chem., Int. Ed.* **2010**, *49*, 6058–6082.
- (4) Tozawa, T.; Jones, J. T. A.; Swamy, S. I.; Jiang, S.; Adams, D. J.; Shakespeare, S.; Clowes, R.; Bradshaw, D.; Hasell, T.; Chong, S. Y.; Tang, C.; Thompson, S.; Parker, J.; Trewin, A.; Bacsa, J.; Slawin, A. M. Z.; Steiner, A.; Cooper, A. I. *Nat. Mater.* **2009**, *8*, 973–978.
- (5) Jin, Y.; Voss, B. A.; Jin, A.; Long, H.; Noble, R. D.; Zhang, W. J. *Am. Chem. Soc.* **2011**, *133*, 6650–6658.
- (6) Mastalerz, M.; Oppel, I. M. *Angew. Chem., Int. Ed.* **2012**, *51*, 5252–5255.
- (7) Sumida, K.; Rogow, D. L.; Mason, J. A.; McDonald, T. M.; Bloch, E. D.; Herm, Z. R.; Bae, T.-H.; Long, J. R. *Chem. Rev.* **2011**, *112*, 724–781.
- (8) Kuwahara, Y.; Kang, D.-Y.; Copeland, J. R.; Brunelli, N. A.; Didas, S. A.; Bollini, P.; Sievers, C.; Kamegawa, T.; Yamashita, H.; Jones, C. W. *J. Am. Chem. Soc.* **2012**, *134*, 10757–10760.
- (9) Thomas, A. *Angew. Chem., Int. Ed.* **2010**, *49*, 8328–8344.
- (10) Vilela, F.; Zhang, K.; Antonietti, M. *Energy Environ. Sci.* **2012**, *5*, 7819–7832.
- (11) Hao, G.-P.; Li, W.-C.; Qian, D.; Wang, G.-H.; Zhang, W.-P.; Zhang, T.; Wang, A.-Q.; Schüth, F.; Bongard, H.-J.; Lu, A.-H. *J. Am. Chem. Soc.* **2011**, *133*, 11378–11388.
- (12) Zhu, X.; Hillesheim, P. C.; Mahurin, S. M.; Wang, C.; Tian, C.; Brown, S.; Luo, H.; Veith, G. M.; Han, K. S.; Hagaman, E. W.; Liu, H.; Dai, S. *ChemSusChem* **2012**, *5*, 1912–1917.
- (13) Ben, T.; Li, Y.; Zhu, L.; Zhang, D.; Cao, D.; Xiang, Z.; Yao, X.; Qiu, S. *Energy Environ. Sci.* **2012**, *5*, 8370–8376.

- (14) Lu, W.; Yuan, D.; Zhao, D.; Schilling, C. I.; Plietzsch, O.; Muller, T.; Bräse, S.; Guenther, J.; Blümel, J.; Krishna, R.; Li, Z.; Zhou, H.-C. *Chem. Mater.* **2010**, *22*, 5964–5972.
- (15) Farha, O. K.; Spokoyny, A. M.; Hauser, B. G.; Bae, Y.-S.; Brown, S. E.; Snurr, R. Q.; Mirkin, C. A.; Hupp, J. T. *Chem. Mater.* **2009**, *21*, 3033–3035.
- (16) Furukawa, H.; Yaghi, O. M. *J. Am. Chem. Soc.* **2009**, *131*, 8875–8883.
- (17) Dawson, R.; Stockel, E.; Holst, J. R.; Adams, D. J.; Cooper, A. I. *Energy Environ. Sci.* **2011**, *4*, 4239–4245.
- (18) Dawson, R.; Adams, D. J.; Cooper, A. I. *Chem. Sci.* **2011**, *2*, 1173–1177.
- (19) Katsoulidis, A. P.; Kanatzidis, M. G. *Chem. Mater.* **2011**, *23*, 1818–1824.
- (20) Ben, T.; Pei, C.; Zhang, D.; Xu, J.; Deng, F.; Jing, X.; Qiu, S. *Energy Environ. Sci.* **2011**, *4*, 3991–3999.
- (21) Chen, Q.; Luo, M.; Hammershøj, P.; Zhou, D.; Han, Y.; Laursen, B. W.; Yan, C.-G.; Han, B.-H. *J. Am. Chem. Soc.* **2012**, *134*, 6084–6087.
- (22) Luo, Y.; Li, B.; Wang, W.; Wu, K.; Tan, B. *Adv. Mater.* **2012**, *24*, 5703–5707.
- (23) Dawson, R.; Stevens, L. A.; Drage, T. C.; Snape, C. E.; Smith, M. W.; Adams, D. J.; Cooper, A. I. *J. Am. Chem. Soc.* **2012**, *134*, 10741–10744.
- (24) Rabbani, M. G.; Reich, T. E.; Kassab, R. M.; Jackson, K. T.; El-Kaderi, H. M. *Chem. Commun.* **2012**, *48*, 1141–1143.
- (25) Rabbani, M. G.; El-Kaderi, H. M. *Chem. Mater.* **2012**, *24*, 1511–1517.
- (26) Rabbani, M. G.; El-Kaderi, H. M. *Chem. Mater.* **2011**, *23*, 1650–1653.
- (27) Mohanty, P.; Kull, L. D.; Landskron, K. *Nat. Commun.* **2011**, *2*, 401.
- (28) Ren, S.; Bojdys, M. J.; Dawson, R.; Laybourn, A.; Khimyak, Y. Z.; Adams, D. J.; Cooper, A. I. *Adv. Mater.* **2012**, *24*, 2357–2361.
- (29) Katekomol, P.; Roeser, J.; Bojdys, M.; Weber, J.; Thomas, A. *Chem. Mater.* **2013**, *25*, 1542–1548.
- (30) Patel, H. A.; Je, S. H.; Park, J.; Chen, D. P.; Jung, Y.; Yavuz, C. T.; Coskun, A. *Nat. Commun.* **2013**, *4*, 1357.
- (31) Zhu, Y.; Long, H.; Zhang, W. *Chem. Mater.* **2013**, *25*, 1630–1635.
- (32) Dawson, R.; Cooper, A. I.; Adams, D. J. *Polym. Int.* **2013**, *62*, 345–352.
- (33) Carta, M.; Malpass-Evans, R.; Croad, M.; Rogan, Y.; Jansen, J. C.; Bernardo, P.; Bazzarelli, F.; McKeown, N. B. *Science* **2013**, *339*, 303–307.
- (34) Zhang, C.; Chen, C.-F. *J. Org. Chem.* **2006**, *71*, 6626–6629.
- (35) Zhang, C.; Liu, Y.; Li, B.; Tan, B.; Chen, C.-F.; Xu, H.-B.; Yang, X.-L. *ACS Macro Lett.* **2011**, *1*, 190–193.
- (36) Du, X.; Sun, Y.; Tan, B.; Teng, Q.; Yao, X.; Su, C.; Wang, W. *Chem. Commun.* **2010**, *46*, 970–972.
- (37) Patel, H. A.; Karadas, F.; Byun, J.; Park, J.; Deniz, E.; Canlier, A.; Jung, Y.; Atilhan, M.; Yavuz, C. T. *Adv. Funct. Mater.* **2013**, *23*, 2270–2276.
- (38) Zhu, X.; Tian, C.; Mahurin, S. M.; Chai, S.-H.; Wang, C.; Brown, S.; Veith, G. M.; Luo, H.; Liu, H.; Dai, S. *J. Am. Chem. Soc.* **2012**, *134*, 10478–10484.
- (39) Liu, F.; Wang, L.; Sun, Q.; Zhu, L.; Meng, X.; Xiao, F.-S. *J. Am. Chem. Soc.* **2012**, *134*, 16948–16950.